Journal of Physics: Conference Series **717** (2016) 012066 doi:10.1088/1742-6596/717/1/012066

Ionization and acceleration of heavy ions in high-Z solid target irradiated by high intensity laser

D Kawahito and Y Kishimoto

Graduate School of Energy Science, Kyoto University, Uji, Kyoto, 611-0011

Abstract. In the interaction between high intensity laser and solid film, an ionization dynamics inside the solid is dominated by fast time scale convective propagation of the internal sheath field and the slow one by impact ionization due to heated high energy electrons coupled with nonlocal heat transport. Furthermore, ionization and acceleration due to the localized external sheath field which co- propagates with Al ions constituting the high energy front in the vacuum region. Through this process, the maximum charge state and then q/A increase in the rear side, so that ions near the front are further accelerated to high energy.

1. Introduction

The development of short pulse high power lasers which intensity reaches to 10^{21}W/cm^2 have opened up new schemes for ion acceleration and associated applications such as hadron radiotherapy, fusion neutron generation, ion driven fast ignition, etc., by choosing the material state properly [1,2]. The relatively lighter elements such as hydrogen, carbon, etc., which easily become fully ionized state with the largest charge-to-mass ratio q/A, and then are accelerated efficiently, have been widely used for such applications. On the basis of these experiences, it is worthwhile to extend the schemes to high energy acceleration of heavy elements, which explores a wider class of application especially related to nuclear physics, e.g., highly charged heavy ion beam, nucleus-nucleus collision and nuclear transmutation, extraction and acceleration of short lived exotic nuclei [3]. In contrast to such lighter elements, heavier ones irradiated by high power laser exhibit complex structure and dynamics dominated by plural physical processes such as ionization and recombination, collision and relaxation, radiation and the transport, etc. These processes have to be taken into account in the analysis simultaneously and self-consistently.

2. Simulation model

We carry out the 2-dimensional simulation for evaluating the ionization and ion acceleration by using EPIC3D (Extended Particle based Integrated Code [4]) which includes atomic processes such as a field ionization and an impact ionization. The field ionization is calculated as tunnel a field ionization process by calculating the electric field per particle based on ADK model [5], and the impact ionization is calculated by the cross-section through a binary collisional process between ion and electron based on BEB model [6]. The field energy loss can be estimated from the energy conservation with the ionization energy, so that we introduce the ionization current calculated from the energy as Joule heating. The simulation capability is set as L_y=14.4 μm (18λ) in the laser propagation direction (-y) and L_x=28.8 μm (36λ) in the transverse direction (-x), where λ (=0.8μm) is a wave length of laser field. In the simulation, the laser peak intensity is assumed to be I=1.0×10^{21} W/cm^2 (a_0=21). The laser field is emitted with P-polarization from the left hand boundary of the simulation domain during the gaussian pulse duration τ=40 fsec and focused into 3 micron diameter to the solid surface. The solid film is

based on an Al (Z=13) atom which is initially located in 3.2 μm < y < 4.0 μm with a thickness l_{Al}=0.8 μm (=λ) and distributed uniformly on the transverse direction. The mass density of the film is 0.675 g/cm^3 which value is 1/4 for the real mass density of Al material, i.e., 2.7 g/cm^3. The initial charge state is set as Al^{1+} assumed the free electrons in the film, so that the initial electron density is n_e/n_{cr}=8.6, where n_{cr} is the cut-off density, i.e., 1.74×10^{21} cm^{-3}. Therefore, the initial penetration length is $\delta_{q=1}=4.35\times10^{-2}$ μm, and that at the fully ionized plasma reaches to $\delta_{q=13}=1.21\times10^{-2}$ μm. In the simulation model, we investigate the ionization dynamics and ion acceleration of Al.

3. Simulation result

3.1 Time history of the ionization process

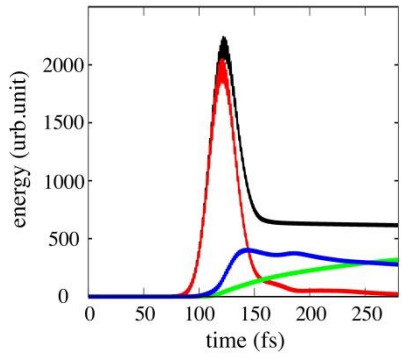

Figure 1. Time history of field (red), electron (blue), ion (gren), and total energy (black).

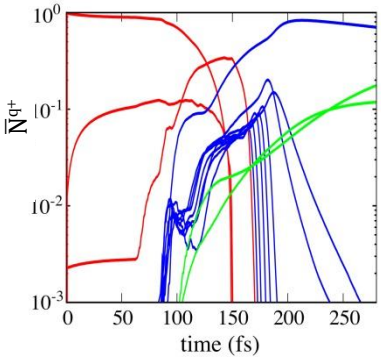

Figure 2. Time history of ion abundance of each charge state, where each lines are M-shell(red), L-shell(blue), and K-shell(green).

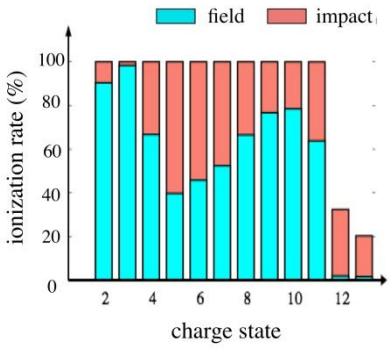

Figure 3. Ionization rate of the the field(blue) and impact(red) for each charge state.

Figure 1 represents the time history of field energy E_f, electron kinetic energy E_e, ion kinetic energy E_i summed up each charge state q (1-13), and total energy E_t (=E_f+E_e+E_i) in the simulation domain, respectively. The laser field is irradiated from the antenna, and then it applies the energy into the simulation domain and the plasma. From t=100 fsec, the both energies of electron and ion start to increase due to the absorption from the laser field with approaching the time of the peak laser intensity (t=120 fsec). After the laser ceases, the electron energy saturates at t=135 fsec and then decrease gradually. A part of field energy remains in the simulation domain as the sheath field which generated by the charge separation between the high energy electrons and ion surface. Then, the ion energy keeps increasing due to the energy transfer from that of the electrons and the field to that of the ions, i.e., sheath ion acceleration.

In this process, we found the two kind of rapid ionization dynamics as seen in Figure 2. Fig.2 shows the ion abundance $\bar{N}^{q+}$ for each charge state of Al in logarithmic scale. Here $\bar{N}^{q+}$ is determined as N^{q+}/N_{ion}, where N^{q+} is ion number for each charge state, and N_{ion} is total ion number. After the laser field hits the surface of the film, the ionization in M-shell electrons proceeds gradually from the initial charge state Al^{1+} until t=80 fsec. Then, the first rapid ionization starts to proceed for L-shell electrons, and the abundance of Al^{11+} which is the final state of the L-shell reaches to $\bar{N}^{11+}$=0.08. The increase of the abundance with the L-shell electrons saturates from t=100 fsec, and the inner ionization to Al^{12+} and Al^{13+} starts to increase gradually. At t=115 fsec, the second rapid ionization takes place from the lower charge state, and the population of ions with charge state in M- and L-shell mostly transits to Al^{11+}, i.e., the ionization state is held in the final charge state of L-shell due to the ionization potential gap between L- and K- shell. The abundance of Al^{11+} reaches $\bar{N}^{11+}$=0.9 at t=200 fsec and then decrease gradually while that of inner charge state: Al^{12+} and Al^{13+} keeps increasing with slower time scale than the other ionization process.

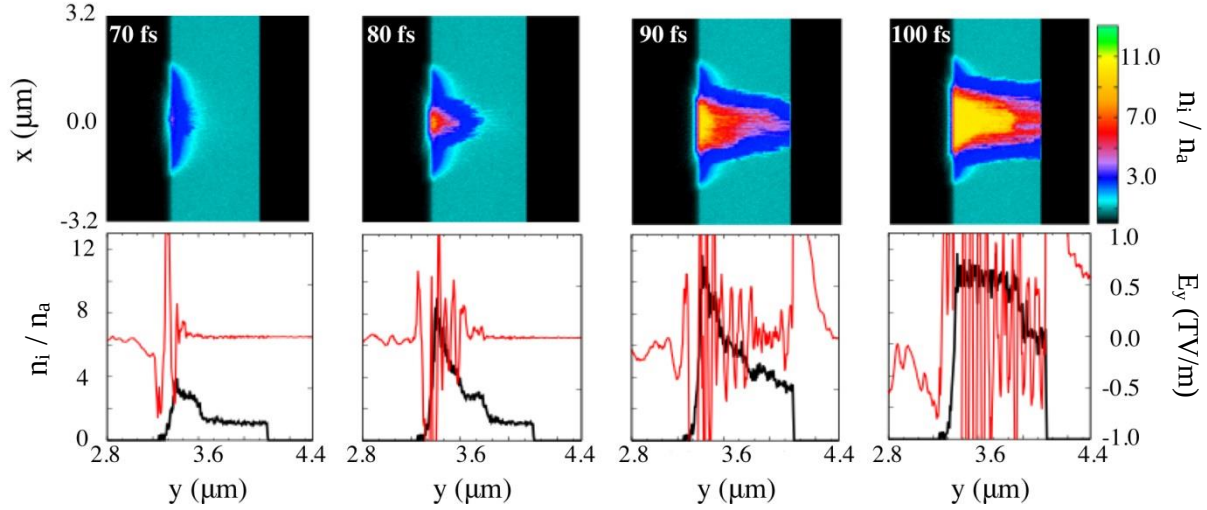

Figure 4. (a) Normalized ion density n_i/n_{av}in 2-dimentional domain at representative times, where n_i is the ion charge density, and n_a is the initial atom density, and (b) the profile of n_i/n_a and the electric field Ey on x=0 at same times to (a)

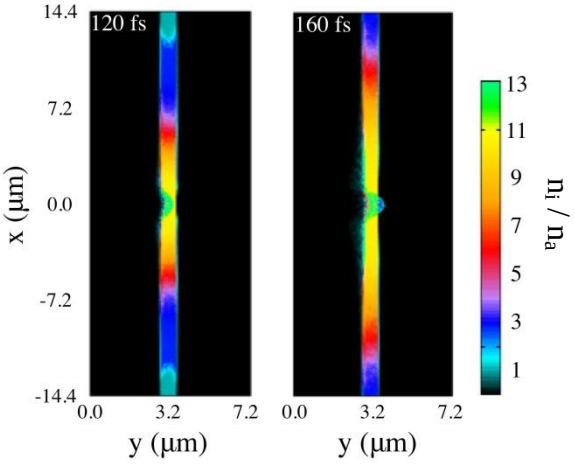

Figure 5. Normalized ion density n_i/n_a in 2-dimentional domain at t=120 fs and t=160 fs.

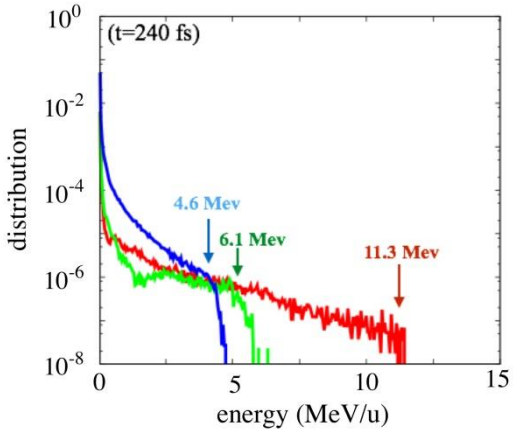

Figure 6. Ion energy distributions for the charge state q=11(blue). q=12(green), and q=13(red)

We also evaluate the difference between the field and the impact as seen in figure 3. Fig.3 shows the ionization rate of the field and the impact component for each charge state until t=250 fsec when the laser has already ceases from the simulation domain. In outer shell, i.e., M-shell, the field ionization takes place dominantly due to the laser field, and the rate reaches to 94.6 % which value is averaged from q=2 to q=3. The impact ionization proceeds only 5.6 %, i.e., the additional rate is 100. In L-shell, the field ionization rate decreases to averagely 40.4 %. Instead of that, the impact ionization rate increases due to the increase of the collisional frequency depended on the ionization degree, and the rate reaches to 59.6 % with slower time scale than that of the field. Finally, in inner-shell, i.e., K-shell, the impact components become dominant rate while that of the field is less than the 1%, however the total ionization proceed to only 25 % of the film. In this case, the ionization loss is estimated from the ionization degree, and the rate is only 0.1% compared with the laser energy. Thus, the ionization loss is negligible for the investigating the dynamics.

3.2 Spatial ionization structure and ion acceleration

Figure 4 represents (a) the normalized ion density n_i/n_a in the region of -3.2 μm < x < 3.2 μm and 2.8 μm < y < 4.4 at representative times, where n_i is the ion charge density, and n_a is the initial atom densi-

ty, i.e., that shows the charge state as far as ions remain, and (b) the profile of n_i/n_a and the electric field E_y on x=0 at same times to (a). The ionization proceeds only around the front surface due to the cut-off of the laser until t=70 fsec. Then, the ionization front starts to propagate to the inside of the film with the electric field E_y as seen in Fig.4 (a) and (b). This transition is driven by the propagation of the fast electron bunches generated by the J×B heating [7]. The electron bunch is accelerated to the relativistic region at the front surface and injected to the inside of the film every twice of the laser frequency. The return current is also excited for the current neutralization with the bunch, and the solitary electric field at the front of bunch and the plasma wave behind that are generated for propagation direction by the charge separation inside the film [8]. Therefore, the field ionization to Al^{11+} takes places with the propagation of the electric fields E_y with the bunch as the first ionization dynamics. The ionization velocity is v_f=0.8c which is almost same as the averagely bunch velocity. After the electrons reach to the rear surface, the sheath field is generated by the charge separation between the ion surface and the electron bunches. The electrons behind of that are reflected by the sheath field to the inside of the film and recirculate between the front and the rear surface with the initial scattering angle. So that, the electrons spread to the transverse direction over the laser spot area with the ionization to Al^{11+} as seen in Figure 5, which is the same as Fig. 4 (a) in the whole region. Around the laser spot area, the field ionization proceeds due to the electron bunches with the electric field as discussed in the above. However, the amplitude of the electric field gradual decreases due to the electron diffusion with the spread to the transverse direction, and the impact ionization rate changes larger than that of the field as second rapid ionization dynamics. Therefore, the velocity of the ionization to Al^{11+} for transverse direction is decelerated to averagely v_f=0.6c compared with the first one. Additional to these rapid ionization processes, the ionization to Al^{12+} and Al^{13+} takes place due to the sheath field on the each surface and the collision around the laser spot area. So that, the charge states of accelerated ion are decided more than Al^{11+} through these ionization processes and extracted from the film.

The multi charged ions are accelerated by the sheath field generated on the both surfaces. The peak amplitude of the sheath field reaches to 35 TV/m which is same order to the laser peak amplitude, so that the ionizations to Al^{12+} and Al^{13+} proceed due to the field ionization from the charge state of the bulk Al^{11+}. Then, the ions are accelerated and extracted to the vacuum region with the dependence of its charge to mass ratio as seen in Figure 6 which represents the ion energy distribution for each charge state. The ions of fully ionized state (Al^{13+}) with the largest charge to mass ratio is accelerated most efficiently in the Al, and then the maximum ion energy reaches to 11.3 MeV/u. On the other hand, the ion energy of Al^{11+} and Al^{12+} reaches to 4.6 MeV/u and 6.1 MeV/u which is less than the dependence of the charge to mass ratio compared with that of Al^{13+}. Therefore, the sheath amplitude for a lower charge state becomes smaller than that for Al^{13+} in the outside than the laser spot area.

In the interaction between such high intensity laser and the solid film of Al, the ionization dynamics with the field and the impact is mainly driven by the electron transport and decide the charge state of accelerated ions. Therefore, we will perform the simulation for higher-Z elements including the other atomic process such as recombination, radiation, etc.

Referencce

[1] H. Daido, M. Nishiuchi, AS.Pirozhkov, Rep.Proq.Phys., **75**, 056401(2012)
[2] Y. Kishimoto, T. Masaki, *et al.*, Phys.Plasmas. **9**, 589(2002)
[3] M. Nishiuchi, H. Sakaki, *et al.*, Phys. Plasmas. **22**, 033107(2015)
[4] T. Masaki, Y. Kishimoto, J. Plasma Fusion Res., **81**, 643(2005)
[5] M. V. Ammosov, et al, Sov. Phys. JETP **64**, 1191 (1986)
[6] Y. K. Kim and M. E. Rudd, Phys. Rev. A **50**, 3954 (1994)
[7] W. L. Kruer and Kent Estabrook., Phys. Fluid **28**,430(1985)
[8] V. T. Tickhonchuk, Phys. plasmas **9**, 4 (2002)